

High-precision absolute distance measurement using dual-laser frequency scanned interferometry under realistic conditions

Hai-Jun Yang*, Sven Nyberg, Keith Riles

Department of Physics, University of Michigan, Ann Arbor, MI 48109, USA

Received 25 December 2006; received in revised form 22 February 2007; accepted 24 February 2007

Available online 6 March 2007

Abstract

In this paper, we report on new high-precision absolute distance measurements performed with frequency scanned interferometry using a pair of single-mode optical fibers. Absolute distances were determined by counting the interference fringes produced while scanning the frequencies of the two chopped lasers. High-finesse Fabry–Perot interferometers were used to determine frequency changes during scanning. Dual lasers with oppositely scanning directions, combined with a multi-distance-measurement technique previously reported, were used to cancel drift errors and to suppress vibration effects and interference fringe uncertainties. Under realistic conditions, a precision about $0.2\ \mu\text{m}$ was achieved for a distance of $0.41\ \text{m}$. With a precision that exceeds requirements, the frequency scanned interferometry is a promising high-precision optical alignment technique for International Linear Collider silicon tracker detector.

© 2007 Elsevier B.V. All rights reserved.

PACS: 07.60.-j; 07.60.Vg; 42.62.-b; 29.40.Gx

Keywords: Frequency scanned interferometry; Absolute distance measurement; Optical alignment system; International Linear Collider; Silicon detector

1. Introduction

We reported previously on single-laser measurements of absolute distance with a frequency scanned interferometry (FSI) apparatus, carried out under controlled laboratory conditions [1]. Here we report on dual-laser measurements carried out under less favorable conditions, more representative of the interior of a high energy physics detector at a collider. The motivation for these studies is to design a novel optical system for quasi-real time alignment of tracker detector elements used in High Energy Physics (HEP) experiments. Fox-Murphy et al. from Oxford University reported their design of a FSI for precise alignment of the ATLAS Inner Detector [2–4]. Given the demonstrated need for improvements in detector performance, we plan to design and prototype an enhanced FSI system to be used for the alignment of tracker elements in the next generation of electron–positron International

Linear Collider (ILC) detectors [5,6]. Current plans for future detectors require a spatial resolution for signals from a tracker detector, such as a silicon microstrip or silicon drift detector, to be approximately $7\text{--}10\ \mu\text{m}$ [7]. To achieve this required spatial resolution, the measurement precision of absolute distance changes of tracker elements in one dimension should be no worse than about $1\ \mu\text{m}$. Simultaneous measurements from hundreds of interferometers will be used to determine the three-dimensional positions of the tracker elements. The FSI method described here allows these simultaneous measurements to be carried out with a single pair of scanning lasers, providing a simple and robust alignment monitoring system for an ILC detector.

Detectors for HEP experiment must usually be operated remotely for safety reasons because of intensive radiation, high voltage or strong magnetic fields. In addition, precise tracking elements are typically surrounded by other detector components, making access difficult. For practical HEP application of FSI, optical fibers for light delivery and return are therefore necessary. The power of front-end

*Corresponding author. Tel.: +1 734 764 3407; fax: +1 734 936 6529.
E-mail address: yhj@umich.edu (H.-J. Yang).

electronics depends on the event occupancy levels and trigger rates during the collider and detector operation. It is possible that the temperature distribution between heat sources and cooling system will vary enough to cause significant shape changes of the silicon detector in a relatively short period of time. Hence, it is critical to design a high precision optical alignment system that performs well under unfavorable environmental conditions.

Absolute distance measurements using FSI under controlled conditions have been reported previously [8–13] by other research groups. Another proposed method for absolute distance measurement with comparable expected precision is based on a phase-stabilized femtosecond laser, using combined time-of-flight information and coherent, fringe-resolved interferometry [14].

The University of Michigan group has constructed several demonstration FSI systems with the laser light transported by air or single-mode optical fiber, using single-laser and dual-laser scanning techniques for initial feasibility studies. Absolute distance was determined by counting the interference fringes produced while scanning the laser frequency. The main goal of the demonstration systems has been to determine the potential accuracy of absolute distance measurements that could be achieved under both controlled and realistic conditions. Secondary goals included estimating the effects of vibrations and studying error sources crucial to the absolute distance accuracy. Two multiple-distance-measurement analysis techniques were developed to improve distance precision and to extract the amplitude and frequency of vibrations. Under well controlled laboratory conditions, a measurement precision of ~ 50 nm was achieved for absolute distances ranging from 0.1 to 0.7 m by using the first multiple-distance-measurement technique (slip measurement window with fixed size) [1]. The second analysis technique (slip measurement window with fixed start point) has the capability to measure vibration frequencies ranging from 0.1 to 100 Hz with amplitude as small as a few nanometers, without a *priori* knowledge [1]. The multiple-distance-measurement analysis techniques are well suited for reducing vibration effects and uncertainties from fringe and frequency determination, but do not handle well the drift errors such as from thermal effects.

The dual-laser scanning technique was pioneered by the Oxford group for alignment of the ATLAS Semi-conductor tracker; it was demonstrated that precisions of better than 0.4 and 0.25 μm for distances of 0.4 and 1.195 m, respectively [3]. In our recent studies, we combine our multi-distance-measurement analysis technique (slip measurement window with fixed size) reported previously with the dual-laser scanning technique to improve the absolute distance measurement precision. The multi-distance-measurement technique is effective in reducing uncertainties from vibration effects and interference fringe determination, while the dual-laser scanning allows for cancellation of drift errors. We report here on resulting

absolute distance measurement precisions under more realistic conditions than in our previous, controlled-environment measurements.

2. Principles

We begin with a brief summary of the principles of FSI and our single-laser measurement technique. The intensity I of any two-beam interferometer can be expressed as $I = I_1 + I_2 + 2\sqrt{I_1 I_2} \cos(\phi_1 - \phi_2)$, where I_1 and I_2 are the intensities of the two combined beams, and ϕ_1 and ϕ_2 are the phases. Assuming the optical path lengths of the two beams are D_1 and D_2 , the phase difference is $\Phi = \phi_1 - \phi_2 = 2\pi(D_1 - D_2) \times (v/c)$, where v is the optical frequency of the laser beam, and c is the speed of light.

For a fixed path interferometer, as the frequency of the laser is continuously scanned, the optical beams will constructively and destructively interfere, causing fringes. The number of fringes ΔN is $\Delta N = D\Delta v/c$, where D is the optical path difference (OPD) between the two beams, and Δv is the scanned frequency range. The OPD (for absolute distance between beamsplitter and retroreflector) can be determined by counting interference fringes while scanning the laser frequency.

If small vibration and drift errors $\varepsilon(t)$ occur during the laser scanning, then $\Phi(t) = 2\pi \times [D_{\text{true}} + \varepsilon(t)] \times v(t)/c$, $\Delta N = [\Phi(t) - \Phi(t_0)]/2\pi = D_{\text{true}}\Delta v/c + [\varepsilon(t)v(t)/c - \varepsilon(t_0)v(t_0)/c]$. Assuming $v(t) \sim v(t_0) = v$ and $\Delta\varepsilon = \varepsilon(t) - \varepsilon(t_0)$, the measured distance can be written as,

$$D_{\text{measured}} = \Delta N/(\Delta v/c) = D_{\text{true}} + \Delta\varepsilon \times \Omega. \quad (1)$$

where Ω is a magnification factor: $\Omega = v/\Delta v$.

3. Demonstration system of FSI

A schematic of the FSI system with a pair of optical fibers is shown in Fig. 1. The light sources are two New Focus Velocity 6308 tunable lasers (Laser 1–665.1 nm $< \lambda < 675.2$ nm; Laser 2–669.2 nm $< \lambda < 679.3$ nm). Two high-finesse (> 200) Thorlabs SA200 Fabry–Perot are used to measure the frequency range scanned by the laser. The free spectral range (FSR) of two adjacent Fabry–Perot peaks is 1.5 GHz, which corresponds to 0.002 nm. A Faraday Isolator was used to reject light reflected back into the lasing cavities. The laser beams were coupled into a single-mode optical fiber with a fiber coupler. Data acquisition is based on a National Instruments DAQ card capable of simultaneously sampling four channels at a rate of 5 MS/s/ch with a precision of 12-bits. Omega thermistors with a tolerance of 0.02 K and a precision of 0.01 mK are used to monitor temperature. The apparatus is supported on a damped Newport optical table.

The beam intensity coupled into the return optical fiber is very weak, requiring ultra-sensitive photodetectors for detection. Given the low light intensity and the need to split into many beams to serve a set of interferometers, it is vital

to increase the geometrical efficiency. To this end, a collimator is built by placing an optical fiber in a ferrule (1 mm diameter) and gluing one end of the optical fiber to a GRIN lens. The GRIN lens is a 0.25 pitch lens with 0.46 numerical aperture, 1 mm diameter and 2.58 mm length which is optimized for a wavelength of 630 nm. The density

of the outgoing beam from the optical fiber is increased by a factor of approximately 1000 by using a GRIN lens. The return beams are received by another optical fiber and amplified by a Si femtowatt photoreceiver with a gain of 2×10^{10} V/A.

4. Dual-laser scanning technique

A dual-laser FSI system was built in order to reduce drift error and slow fluctuations occurring during the laser scan, as shown in Fig. 1. Two lasers are operated simultaneously; the two laser beams are coupled into one optical fiber but isolated by using two choppers. The advantage of the dual-laser technique comes from cancellation of systematic uncertainties, as indicated in the following. For the first laser, the measured distance $D_1 = D_{\text{true}} + \Omega_1 \times \Delta \varepsilon_1$, and $\Delta \varepsilon$ is drift error during the laser scanning. For the second laser, the measured distance $D_2 = D_{\text{true}} + \Omega_2 \times \Delta \varepsilon_2$. Since the two laser beams travel the same optical path during the same period, the drift errors $\Delta \varepsilon_1$ and $\Delta \varepsilon_2$ should be very comparable. Under this assumption, the true distance can be extracted using the formula $D_{\text{true}} = (D_2 - \rho \times D_1) / (1 - \rho)$, where, $\rho = \Omega_2 / \Omega_1$, the ratio of magnification factors from two lasers. If two similar lasers scan the same range in opposite directions simultaneously, then $\rho \simeq -1.0$, and D_{true} can be written as

$$D_{\text{true}} = (D_2 - \rho \times D_1) / (1 - \rho) \simeq (D_2 + D_1) / 2.0. \quad (2)$$

Unfortunately, there are disadvantages too in the dual-laser technique. Because the laser beams are isolated by periodic choppers, only half the fringes are recorded for each laser, degrading the distance measurement precision, as shown in Fig. 2. Missing fringes during chopped intervals for each laser must be recovered through robust interpolation algorithms. Based on our studies, the number of interference fringes in a time interval with fixed number of Fabry–Perot peaks is stable. The measured number of fringes is typically within 0.3 of the expected

Dual-Laser Frequency Scanned Interferometer

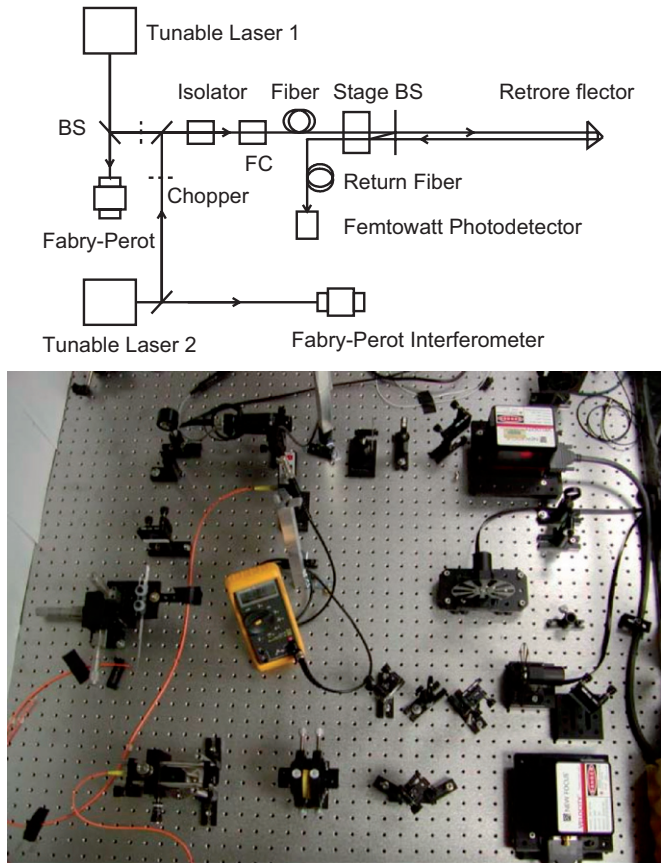


Fig. 1. Schematic of the dual-laser FSI system.

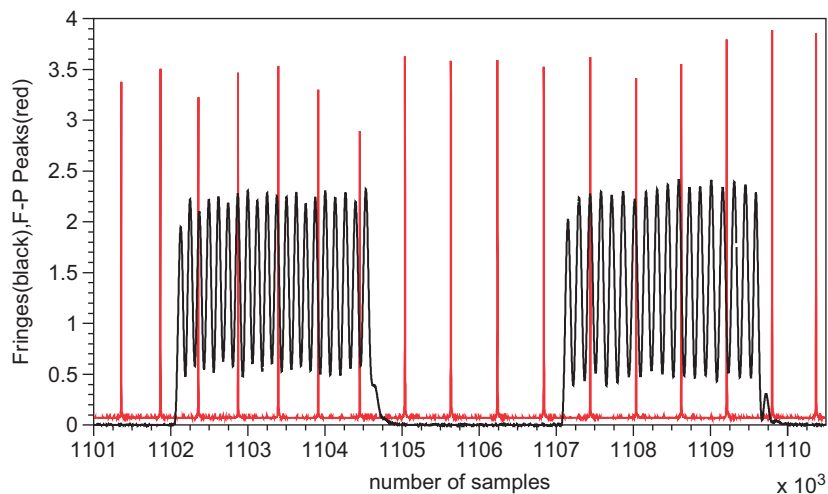


Fig. 2. Sample fringes and Fabry–Perot peaks from the first laser with chopping and with the second laser turned off.

fringe number, which enables us to estimate the number of fringes in the chopper-off slots (when the laser beam is blocked by the chopper). In order to determine the number of fringes in one chopper-off slot, we need to identify two Fabry–Perot peaks within the two adjacent chopper-on slots closest to the chopper-off slot. If the fringe phases at the two Fabry–Perot peaks positions are $M + \Delta M$ and $J + \Delta J$, where M and J are integers, ΔM and ΔJ are fraction of fringes; then the number of true fringes can be determined by minimizing the quantity $|\mathcal{N}_{\text{correction}} + (J + \Delta J) - (M + \Delta M) - \mathcal{N}_{\text{expected-average}}|$, where $\mathcal{N}_{\text{correction}}$ is an integer used to correct the fringe number in the chopper off slot, $\mathcal{N}_{\text{expected-average}}$ is the expected average number of fringes, based on a full laser scanning sample shown in Fig. 3.

For the example shown in Fig. 2, the number of Fabry–Perot intervals is 5 in the chopper-off slot, so the expected number of fringes shown in the second plot of Fig. 3 is about 20.6; The number of fringes measured in the chopper-off slot is 3.55, $\mathcal{N}_{\text{correction}}$ is 17 based on the above formula, meaning 17 fringes are missed in the chopper-off slot. So the total number of fringes in this slot is 20.55, well within the expected range 20.6 ± 0.3 .

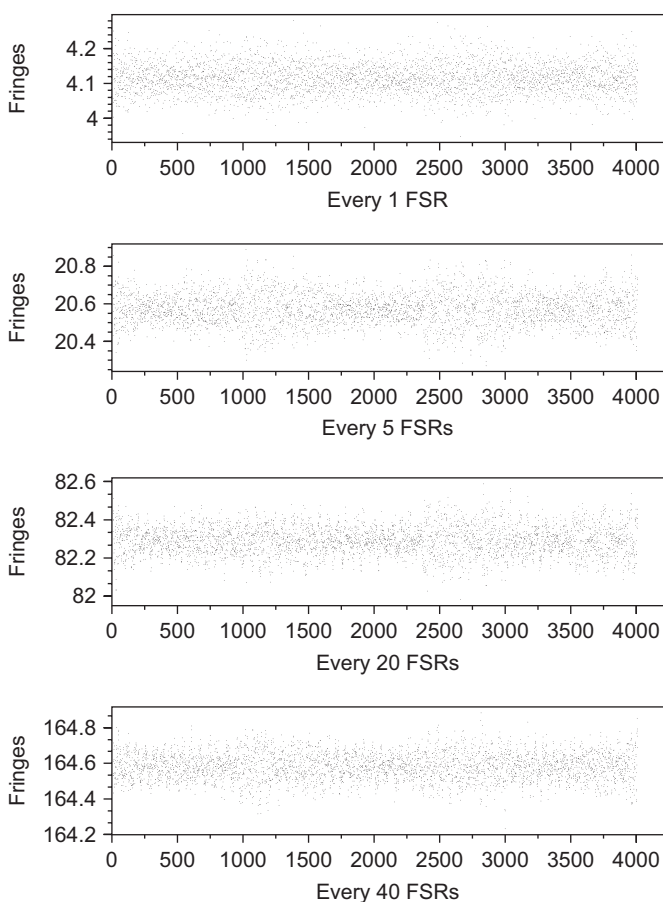


Fig. 3. The number of fringes for fixed numbers of Fabry–Perot intervals (1,5,20,40) from full scan data.

5. Absolute distance measurement

Under realistic and deliberately generated hostile conditions of air flow and vibration, 40 dual-laser-scan data samples were collected as listed in the following. The “box” refers to a nested enclosure of plexiglass box covering the optical table and PVC pipe surrounding the interferometer beam path, used in previous measurements [1] to isolate the interferometer from environmental fluctuations. Both the cover of the box and the pipe are removed for the measurements described here.

- with open box (10 scans) and ambient room environment,
- with open box and a chassis cooling fan (9 cm diameter) blowing air toward the beam splitter about 0.93 m away from the retroreflector along the FSI (10 scans),
- with open box and fan off (10 scans),
- with open box and a vibration source (10 scans), with a PI piezoelectric translator (P-842.10) used to generate controlled vibrations with frequency of 1 Hz and amplitude of about $0.15 \mu\text{m}$. (Ten scans were collected, but 2 scans were found to have suffered a power glitch on one laser, invalidating the distance reconstructions. These 2 scans were excluded from the analysis.)

To verify correct tracking of large thermal drifts, another set of scans was carried out after remounting the interferometer on a $1' \times 2' \times 0.5''$ Aluminum breadboard (Thorlabs) and placing the breadboard on a heating pad (Homedics). Twenty dual-laser-scan data samples with the heating pad off and on were collected as listed in the following:

- with open box and the heating pad off (10 scans with one scan excluded because of a power glitch),
- with open box and the heating pad on (10 scans).

The two lasers were scanned oppositely with scanning speeds of $\pm 0.4 \text{ nm/s}$ and a full-scan time of 25 s. The choppers have two blades with operation frequency of 20 Hz for these dual-laser scans. The measured precision is found to vary from about 3–11 μm if we use the fringes of these data samples from only one laser for a measured distance of 0.41 m. The single-laser multi-distance-measurement technique does not improve the distance measurement precision in open box data because drift error dominates. If we combine the measured distances from two lasers using Eq. (2), then the dual-laser measurement precision is found to be about $0.2 \mu\text{m}$ for a number of multi-distance-measurements larger than 500, as shown in Fig. 4 and Table 1. From Table 1, it is apparent that if we use fewer distance measurements/scan or a single-distance-measurement, then the measured precision worsens significantly. Combining the dual-laser scanning technique and multi-distance-measurement technique ensures that

vibrations, fringe uncertainties and drift errors are greatly suppressed.

Under nearly identical conditions, the measured distances from laser 1 and laser 2 are slightly different, as

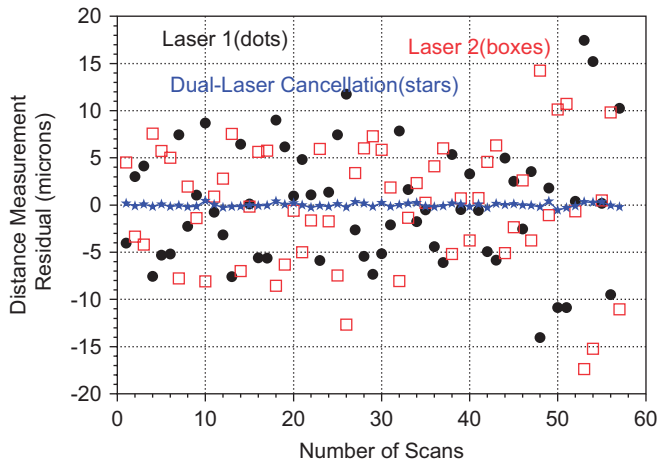


Fig. 4. Distance measurement residuals versus number of scans for dual-laser scanning data. The measurement residuals refer to differences between measured distances and the arithmetic averages of measured distances from each set of 10 scans under same conditions. The number of distance measurements/scan is 2000 for these residuals. Dots show distance measurement residuals from laser 1 and boxes from laser 2. The distance measurement residuals with dual-laser cancellation are shown in stars.

expected from their slightly different FSRs (taken to be 1.5 GHz for the distance measurements) of the two Fabry–Perot interferometers. Since a high precision wavemeter is not available in our laboratory currently, we cannot calibrate the FSRs of two Fabry–Perot interferometers precisely. Instead, we use the measured distances from two lasers to determine the ratio (1.0005928) between the FSRs of the two Fabry–Perot interferometers, and then normalize all measured distances from the second laser using the same factor. This correction method was validated previously with a different interferometer configuration by comparing the normalization factor to that inferred from measuring the transmission peaks of the two Fabry–Perot interferometers when monitoring the same laser. That check was limited in precision, however, to no better than 4 ppm.

In order to verify the correct tracking of large thermal drifts, we placed a heating pad on the Aluminum breadboard. Thermistors are taped to the breadboard but electrically isolated. The true temperature of the breadboard is inferred to be the $0.6 \pm 0.1^\circ\text{C}$ higher than the measured temperature from extrapolation of temperature gradient from three external thermistors. Four independent tests with different temperature increases are made, the results are shown in Table 2. Each test has 20 dual-laser scans for the distance measurement before (10 scans) and after (10 scans) the temperature increase. The expected

Table 1

Distance measurement precisions using the multiple-distance-measurement and dual-laser scanning techniques

Data	Scans	Conditions	Distance (cm) from dual-laser	Precision (μm) for multi-dist.-meas./scan					
				2000	1500	1000	500	100	1
L1	10	Open box	–	5.70	5.73	6.16	6.46	5.35	6.64
L2	10	Open box	–	5.73	5.81	6.29	6.61	5.66	6.92
L1 + L2	10	Open box	41.13835	0.20	0.19	0.18	0.21	0.39	1.61
L1	10	With fan on	–	5.70	4.91	3.94	3.49	3.29	3.04
L2	10	With fan on	–	5.70	5.19	4.23	3.78	3.21	6.07
L1 + L2	10	With fan on	41.13841	0.19	0.17	0.20	0.22	0.31	3.18
L1	10	With fan off	–	6.42	5.53	4.51	3.96	4.41	3.36
L2	10	With fan off	–	6.81	5.93	4.86	4.22	4.63	5.76
L1 + L2	10	With fan off	41.13842	0.20	0.20	0.26	0.19	0.27	2.02
L1	8	With vibration on ^a	–	4.73	4.82	3.60	3.42	4.62	8.30
L2	8	With vibration on	–	4.72	4.66	3.66	3.65	4.63	5.56
L1 + L2	8	With vibration on	41.09524	0.17	0.21	0.17	0.15	0.39	1.75
L1	9	With heating pad off ^b	–	3.88	3.90	3.57	3.65	3.28	3.84
L2	9	With heating pad off	–	4.01	4.01	3.64	3.55	3.25	4.66
L1 + L2	9	With heating pad off	40.985122	0.14	0.14	0.11	0.12	0.19	1.86
L1	10	With heating pad on	–	11.39	11.15	10.05	7.44	6.24	5.04
L2	10	With heating pad on	–	11.42	11.21	10.23	7.39	6.47	6.30
L1 + L2	10	With heating pad on	40.987189	0.32	0.19	0.20	0.19	0.20	1.24

All 57 scans are for dual-laser scanning data. Rows starting with L1 or L2 show results using fringes and Fabry–Perot information from the 1st or 2nd laser only to make distance measurement, L1 + L2 shows results by combining measurement distances from both lasers to cancel the drift errors.

^aAttaching the piezoelectric transducer required disturbing the position of the retroreflector.

^bThe last two sets of data were taken four months after the first four data sets, the beamsplitter and retroreflector are moved from optical table to the Aluminum breadboard.

Table 2
Expected and measured distance changes versus temperature changes

$\Delta T(^{\circ}\text{C})$	$\Delta R_{\text{expected}}(\mu\text{m})$	$\Delta R_{\text{measured}}(\mu\text{m})$
6.7 ± 0.1	62.0 ± 0.9	61.72 ± 0.18
6.9 ± 0.1	64.4 ± 0.9	64.01 ± 0.23
4.3 ± 0.1	39.7 ± 0.9	39.78 ± 0.22
4.4 ± 0.1	40.5 ± 0.9	40.02 ± 0.21

distance changes agree well with the measured distance changes due to thermal extension. The uncertainty of the expected distance change comes mainly from the large error in temperature measurement of the Aluminum breadboard. Temperature fluctuations are found to be about 0.1–0.3 °C in half a minute with the heating pad on (low–high level), about 2–6 times larger than the temperature fluctuations with open box and the heating pad off.

In order to verify the distance measurement from FSI, a pizeoelectric transducer (P-842.10 from PI, with 20% tolerance) was used to generate controlled position shifts of the retroreflector. For instance, for an input voltage of 13.13 V, the expected distance change is $1.97 \pm 0.39 \mu\text{m}$. The measured distance change under controlled conditions is $2.23 \pm 0.07 \mu\text{m}$, in good agreement.

6. Error estimation

Based on the error estimation we reported previously [1], the distance measurement statistical uncertainty is about $0.05 \mu\text{m}$ under well controlled, closed box conditions. For the dual-laser scanning technique, only about 40% of the independent fringe measurements can be used in the multi-distance-measurement, giving an expected statistical uncertainty of the distance measurement from each laser of no better than about $0.05 \times \sqrt{1/0.4} \sim 0.08$ microns. The measurement errors from laser 1 and laser 2 propagate to the final distance measurement using Eq. (2), leading to a corresponding error of about $0.08 * \sqrt{2}/2 \sim 0.057 \mu\text{m}$.

Since manual scan starts give laser start times that may differ by as much as 0.5–1.0 s, expected differences in drift errors are expected to differ by as much as 2–4%. Typically, the drift errors from single laser are found to be about 3–11 μm for different samples under open-box conditions, as shown in Table 1; so the expected uncertainty ranges from 0.03 to 0.22 μm .

Combining all above errors, the expected distance measurement statistical uncertainty ranges as high as 0.23 μm , consistent with the measured variations.

Some other sources can contribute to systematic bias in the absolute distance measurement. The major systematic bias comes from the uncertainty in the FSR of the Fabry–Perot used to determine the scanned frequency range. A high precision wavemeter (e.g. $\Delta\lambda/\lambda \sim 10^{-7}$) was not available for the measurements described here. The systematic bias from the multiple-distance-measurement technique is typically less than 50 nm. The systematic bias

from uncertainties in temperature, air humidity and barometric pressure scale are estimated to be negligible.

7. Conclusion

In this paper, high-precision absolute distance measurements were performed with FSI using dual-laser scanning and multi-distance-measurement techniques. The dual-laser scanning technique is confirmed to cancel drift errors effectively, and the multi-distance-measurement technique is used to suppress the vibration and uncertainties from interference fringe determination. Under realistic conditions, a precision of about $0.2 \mu\text{m}$ was achieved for an absolute distance of 0.41 m. With a precision that exceeds requirements, this achievement confirms that the FSI technique is promising for ILC silicon tracker detector. Next the University of Michigan ILC group will miniaturize the components used in this study and test them to verify that the low-mass requirements of an alignment system can be satisfied. When a silicon detector prototype becomes available, further testing will be conducted.

Acknowledgments

This work is supported by the National Science Foundation and the Department of Energy of the United States.

References

- [1] H.-J. Yang, J. Deibel, S. Nyberg, K. Riles, High-precision absolute distance and vibration measurement using frequency scanned interferometry, *Appl. Opt.* 44 (2005) 3937–3944 (physics/0409110).
- [2] A.F. Fox-Murphy, D.F. Howell, R.B. Nickerson, A.R. Weidberg, Frequency scanned interferometry (FSI): the basis of a survey system for ATLAS using fast automated remote interferometry, *Nucl. Instr. and Meth. A* 383 (1996) 229–237.
- [3] P.A. Coe, D.F. Howell, R.B. Nickerson, Frequency scanning interferometry in ATLAS: remote, multiple, simultaneous and precise distance measurements in a hostile environment, *Meas. Sci. Technol.* 15 (11) (2004) 2175–2187.
- [4] P.A. Coe, An investigation of frequency scanning interferometry for the alignment of the ATLAS semiconductor tracker, Doctoral Thesis, St. Peter's College, University of Oxford, Keble Road, Oxford, United Kingdom, 2001, pp. 1–238.
- [5] (<http://www.linearcollider.org/>).
- [6] H.-J. Yang, S. Nyberg, K. Riles, Frequency scanned interferometry for ILC tracker alignment, ECONF C0508141:ALCPG1310, 2005 (physics/0506197).
- [7] American Linear Collider Working Group (161 authors), Linear Collider Physics, Resource Book for Snowmass 2001, Prepared for the Department of Energy under contract number DE-AC03-76SF00515 by Stanford Linear Collider Center, Stanford University, Stanford, California, hep-ex/0106058, SLAC-R-570, 2001 pp. 299–423.
- [8] J.A. Stone, A. Stejskal, L. Howard, Absolute interferometry with a 670-nm external cavity diode laser, *Appl. Opt.* 38 (28) (1999) 5981–5994.
- [9] D. Xiaoli, S. Katuo, High-accuracy absolute distance measurement by means of wavelength scanning heterodyne interferometry, *Meas. Sci. Technol.* 9 (1998) 1031–1035.

- [10] G.P. Barwood, P. Gill, W.R.C. Rowley, High-accuracy length metrology using multiple-stage swept-frequency interferometry with laser diodes, *Meas. Sci. Technol.* 9 (1998) 1036–1041.
- [11] K.H. Bechstein, W. Fuchs, Absolute interferometric distance measurements applying a variable synthetic wavelength, *J. Opt.* 29 (1998) 179–182.
- [12] J. Thiel, T. Pfeifer, M. Haetmann, Interferometric measurement of absolute distances of up to 40m, *Measurement* 16 (1995) 1–6.
- [13] H. Kikuta, R. Nagata, Distance measurement by wavelength shift of laser diode light, *Appl. Opt.* 25 (1986) 976–980.
- [14] J. Ye, Absolute measurement of a long arbitrary distance to less than an optical fringe, *Opt. Lett.* 29 (2003) 1153–1155.